9340 *Biochemistry* **2009,** *48,* 9340–9346
DOI: 10.1021/bi901417f

BIOCHEMISTRY
including biophysical chemistry & molecular biology
Current Topic

Structural Heterogeneity of 6 M GdmCl-Denatured Proteins: Implications for the Mechanism of Protein Folding[†]

Jui-Yoa Chang*

Research Center for Protein Chemistry, Brown Foundation Institute of Molecular Medicine, and Department of Biochemistry and Molecular Biology, University of Texas, Houston, Texas 77030

Received August 13, 2009; Revised Manuscript Received September 3, 2009

ABSTRACT: An in vitro experiment with protein folding is typically initiated with 6 M GdmCl-denatured proteins, which are generally considered fully unfolded. However, studies conducted by various laboratories have shown that many 6 M GdmCl-denatured proteins are structurally heterogeneous and still retain nativelike residual structures. The extent of conformational heterogeneity of the 6 M GdmCl-denatured protein has significant implications for the folding landscape as well as the interpretation of the observed early stage folding mechanism. Using the method of disulfide scrambling, we are able to gain rough insight into the diverse structural properties of 6 M GdmCl-denatured proteins. It demonstrates that most 6 M GdmCl-denatured proteins are approximately fully denatured, but partially unfolded. Most of them comprise diverse conformational isomers. We review here the cumulative evidence obtained from various laboratories and also provide experimental data obtained in our laboratory.

GDMCL-DENATURED PROTEINS COMPRISE HETEROGENEOUS CONFORMATIONAL ISOMERS AND OFTEN RETAIN RESIDUAL STRUCTURES

Elucidation of the pathway and mechanism of protein folding remains one of the most challenging subjects in structural biology (*1*−*5*). In the vast majority of in vitro studies, folding experiments are typically initiated with 6 M GdmCl (or 8 M urea)-denatured proteins. In the cases of disulfide proteins, native disulfide bonds are usually kept intact (disulfide intact) in the denatured state. GdmCl (6 M)-denatured proteins are generally considered fully unfolded or extensively unfolded. Forty years ago, Tanford (*6*, *7*) showed that 6 M GdmCl-denatured proteins were essentially structureless. However, subsequent research from various groups using more sophisticated techniques has shown that residual structures do persist in many proteins even under strongly denaturing conditions (e.g., 7.5 M GdmCl) (*8*−*15*). NMR and circular dichroism techniques have proven to be particularly useful in comprehensive structural characterization of denatured proteins (*16*−*18*). Denatured structures of barnase (*19*), protein L variant (*8*), *Drosophila melanogaster* (*20*), protein G (*21*), 434 repressor (*9*), ferricytochrome *c* (*22*), staphylococcal nuclease (*11*), α-lactalbumin (*23*, *24*), antichymotrypsin (*25*), SH3 domain (*26*), and fatty acid binding protein (*27*) were reported. A common conclusion obtained from these studies is the persistence of residual hydrophobic clusters and nativelike secondary structures in the denatured state of proteins (*10*, *13*, *15*).

The structure of 6 M GdmCl-denatured protein is relevant to the study of protein folding because there is always concern regarding the conformational heterogeneity of the starting materials and whether they still possess residual secondary structures or hydrophobic clusters. These remaining structures may skew the observation of the early folding mechanism, which is the most crucial event in understanding how protein folding is started (*28*−*36*) and in defining the model of protein folding (*37*, *38*). Therefore, characterization of the structural heterogeneity of 6 M GdmCl-denatured proteins is critically important to the interpretation of the observed protein folding pathway and mechanism. Achieving this will require, among other efforts, the development of methods that would allow quantification of the conformational heterogeneity of denatured protein and isolation of unfolded isomers.

CONFORMATIONAL HETEROGENEITY OF DENATURED PROTEINS CAN BE ASSESSED BY THE METHOD OF DISULFIDE SCRAMBLING

Despite the evidence presented above, analysis and quantification of conformational heterogeneity of denatured proteins are inherently difficult, not only because of their exceedingly large number but also because of their dynamic mobility and interconversion. The method of disulfide scrambling (*39*−*42*) serves to overcome some of these problems. This is achieved by incubation of the native disulfide protein in the alkaline buffer (e.g., pH 8.0−8.4) containing a denaturant (e.g., 1−6 M GdmCl) and a thiol catalyst (e.g., 0.05−0.25 mM β-mercaptoethanol or 0.1−1 mM cysteine). Under these conditions, β-mercaptoethanol or cysteine serves as a catalyst to assist in disulfide shuffling. The native protein (N-protein) denatures and unfolds by scrambling its native disulfide bonds and converts to a mixture of fully oxidized non-native isomers (X-isomers) which are amenable to fractionation, quantification, isolation, and further structural analysis. The number of possible X-isomers is determined by the number of disulfide bonds. For instance, a 3- and 4-disulfide protein can theoretically generate a maximum of 14 and 104 unfolded X-isomers, respectively. All isolated X-isomers may

[†]I acknowledge the support of the Robert Welch Foundation and IsoVax Therapeutics Inc.

*To whom correspondence should be addressed: Institute of Molecular Medicine, 1825 Pressler St., Houston, TX 77030. Telephone: (713) 500-2458. Fax: (713) 500-2447. E-mail: Rowen.Chang@uth.tmc.edu.

 Published on Web 09/03/2009

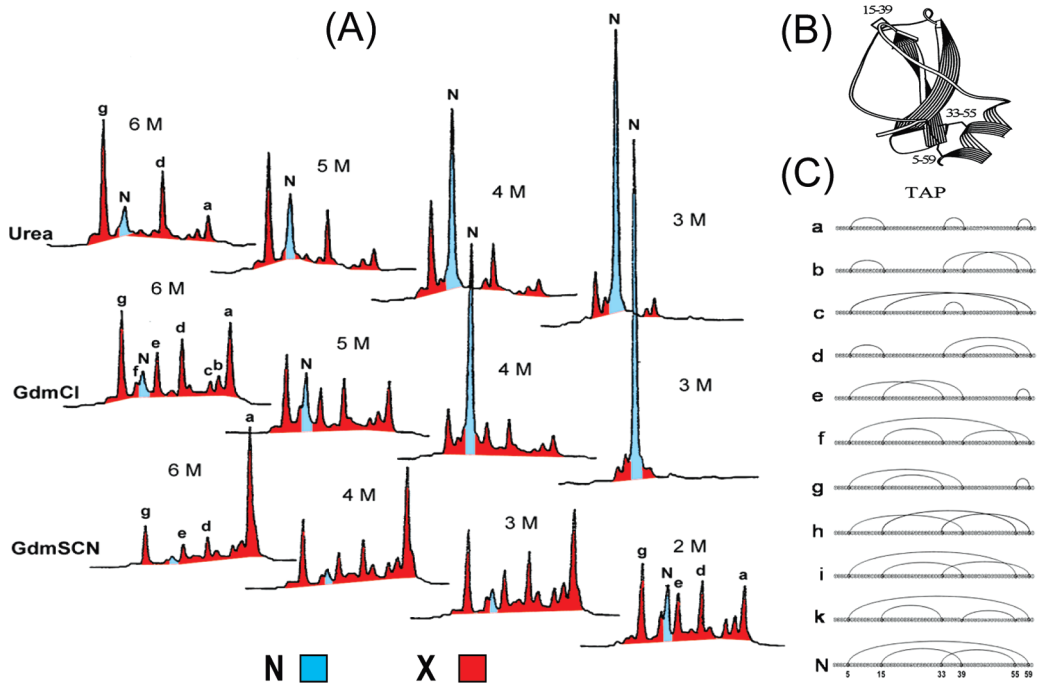

FIGURE 1: (A) Denaturation and unfolding of TAP using the method of disulfide scrambling. Native TAP was incubated in Tris-HCl buffer (0.1 M, pH 8.4) containing 0.2 mM β-mercaptoethanol and increasing concentrations (from 1 to 6 M) of urea, GdmCl, and GdmSCN. The reactions were conducted at 23 °C for 16 h to allow the reaction to reach equilibrium. Unfolded samples were acidified and analyzed directly by HPLC (*40*). Seven major X-TAP isomers (**a**−**g**) were identified as unfolding intermediates. (B) Structure of N-TAP with three native disulfide bonds (*31*). (C) Disulfide connectivity of X-TAP isomers. Three additional X-TAP species (h, i, and k) were identified along the folding pathway of X-TAP-**a** (*56*) (Figure 3).

also refold spontaneously to form the native protein in the alkaline buffer (pH 8.0−8.4) containing a thiol catalyst.

Application of this method is illustrated here with the example of denaturation and unfolding of tick anticoagulant peptide (TAP)[1] (*40*). TAP is a factor Xa specific inhibitor, which contains 60 amino acids and is stabilized by three native disulfide bonds. It is a kunitz-type protease inhibitor structurally homologous to BPTI (*43*). TAP was denatured at increasing concentrations of urea, GdmCl, and GdmSCN. Samples of denatured TAP were analyzed by HPLC (Figure 1) as previously described in ref *40*. The results demonstrate the following. (a) Denatured TAP comprises seven major X-TAP isomers of 14 possible X-isomers. They are designated with lowercase letters (**a**−**g**). Their disulfide structures are given in Figure 1. (b) The structure of denatured TAP (composition of the seven X-TAP isomers) varies significantly under different denaturant strengths. The heterogeneity reaches a maximum at 2−3 M GdmSCN and 6 M GdmCl. (c) X-TAP-**a** is the only isomer with a constant rising recovery that is proportional to the increasing denaturant strength. The recovery of X-TAP-**a** increases from <1 to 23% as the concentration of GdmCl increases from 3 to 6 M. Similarly, it increases from 17 to 60% as the concentration of GdmSCN increases from 2 to 6 M. Thus, X-TAP-**a** was identified as the most unfolded X-isomer of denatured TAP. The recovery of X-TAP-**a** is used to measure the extent of unfolding of denatured TAP. Extrapolation of these data indicates that in theory TAP may become fully unfolded (~100% yield of X-TAP-**a**) at ~10−12 M GdmSCN, an experiment that is unfeasible to execute because of the limited solubility of GdmSCN.

It is relevant to point out that the distribution of X-TAP isomers under denaturing conditions is apparently governed by the thermodynamic free energy state. For instance, under identical conditions in the presence of 6 M GdmCl and a thiol catalyst, the quantitative distribution of X-TAP isomers remains indistinguishable regardless of whether the reaction is initiated from (a) N-TAP by disulfide scrambling as described in the legend of Figure 1, (b) fully reduced R-TAP by oxidative folding (see Figure 5 in ref *55*), or (c) any isolated X-TAP isomer by disulfide scrambling. This property of equilibrium distribution has been similarly demonstrated in the case of hirudin, as shown in Figure 2 (*39*).

It is also important to stress that the structural complexity of a denatured and unfolded protein is enormous. The method of disulfide scrambling serves to facilitate grouping of unfolded isomers that are amenable to fractionation, isolation, and further characterization. It is with almost certainty that each of the X-TAP isomers (including X-TAP-**a**) still has significant conformational freedom and further comprises heterogeneous structures of unfolded TAP. The same should be true for X-isomers produced from other proteins. It is also important to point out that X-TAP-**a** is only a reference structure in defining the relative extent of unfolding of X-TAP isomers. It is not known whether X-TAP-**a** still retains residual structures. Interestingly, none of the four predominant X-TAP isomers (**a**, **d**, **e**, and **g**) allowed under 6 M GdmCl comprises a large disulfide loop linking the cysteines from both N- and C-termini, suggesting that in the extensively denatured state the conformational restriction favors extended linear structures. More compact X-TAP isomers (**f**, **k**, **h**, and **i**) comprising large disulfide loops form at the final stage of the folding process (Figure 3).

CONFORMATIONAL HETEROGENEITY OF 6 M GDMCL-DENATURED PROTEINS REVEALED BY THE TECHNIQUE OF DISULFIDE SCRAMBLING

Using this method, we have investigated the state of denaturation and unfolding of several disulfide proteins at 6 M

[1]Abbreviations: TAP, tick anticoagulant peptide; BPTI, bovine pancreatic trypsin inhibitor.

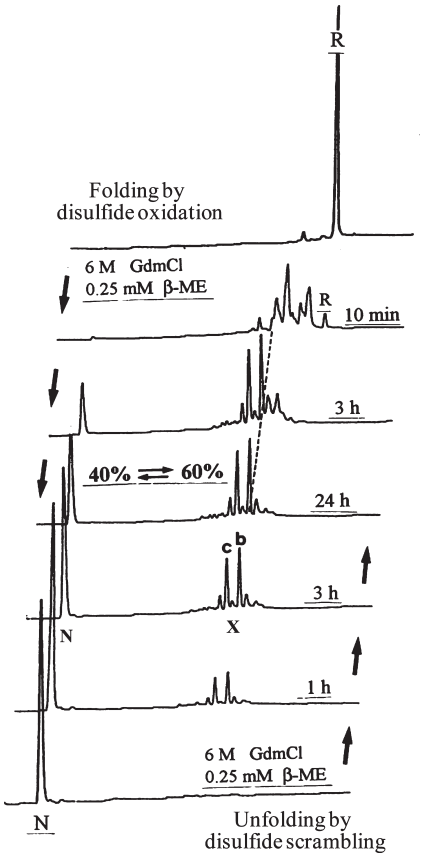

FIGURE 2: Demonstration of the equilibrium distribution of protein X-isomers governed by the free energy state. Hirudin (49 amino acids and three disulfides, a thrombin specific inhibitor) is shown here as an example. At 6 M GdmCl and in the presence of 0.25 mM β-mercaptoethanol, the equilibrium distribution of N-hirudin (40%) and X-hirudin (60%) remains constant, regardless of whether the reaction is initiated from N-hirudin via disulfide scrambling or fully reduced R-hirudin via oxidative folding (*39*). The reactions were conducted at 22 °C in Tris-HCl buffer (0.1 M, pH 8.4). Both reactions reached equilibrium after ~6 h. These experiments revealed that at 6 M GdmCl, only 60% of native hirudin become denatured (Table 1). Note that denatured hirudin comprises two major (**b** and **c**) and three minor fractions of X-hirudin. Each of them contains a single X-hirudin isomer, except for fraction **c** which comprises two X-hirudin isomers (*39*).

GdmCl (*39*−*41*, *44*−*49*). Table 1 gives a rough assessment of the conformational heterogeneity of proteins denatured by 6 M GdmCl. Their structural properties are described by the extent of denaturation, unfolding, and conformational heterogeneity. (a) The extent of denaturation is defined by the conversion of N-protein → X-isomers and is quantified by the recovery of total X-isomers as the percentage of total protein (X vs $X + N$). According to this definition, any isomer that does not have the intact native disulfide bonds is considered denatured. (b) The extent of unfolding is characterized by the composition among X-isomers and is quantified by the recovery of the most extensively unfolded X-isomer as the percentage of total protein. The most extensively unfolded X-isomer is identified by two experiments. During the unfolding experiment, it is the only X-isomer with a steady rise of recovery that is proportional to the increasing strength of the denaturant (*40*, *41*). During the refolding experiment, it is the only X-isomer that flows through all other identified isomers, but not vice versa (*42*). In another word, it is the X-isomer that exhibits the highest free energy. For TAP, the most extensively unfolded isomer is X-TAP-**a** (Figure 1). (c) The extent of heterogeneity is defined by the number of identified X-isomers as the percentage of the maximum possible number of X-isomers. This gives an only rough estimation of the extent of heterogeneity of 6 M GdmCl-denatured proteins. For instance, in the case of denatured TAP, which was found to comprise seven X-isomers, the extent of its conformational heterogeneity is 50% (7 of 14 possible X-isomers). X-Isomers with a recovery of $< 3-5\%$ of the most predominant X-isomer were excluded from the calculation.

The results (Table 1) demonstrate the following. (a) Proteins are not always fully denatured at 6 M GdmCl. Hirudin and BPTI are two notable examples. Only 60% of native hirudin (*39*) and astoundingly less than 2% of native BPTI (*44*) become denatured at 6 M GdmCl. (b) Most 6 M GdmCl-denatured proteins are partially unfolded. Their structures may continue to unfold as the concentration of GdmCl further increases (Figure 1). (c) Most 6 M GdmCl-denatured proteins comprise diverse unfolded isomers. The extent of heterogeneity varies among different proteins. For three-disulfide proteins, we found that their denatured structures usually comprise ~35−50% of the possible X-isomers. For four-disulfide proteins, their conformational heterogeneity is indeed greater than those presented in Table 1. This is due to the exclusion of minor X-isomers from the calculation. For example, 6 M GdmCl-denatured lysozyme (*49*) comprises approximately nine X-isomers (Figure 4); seven minor ones were ignored in the calculation.

STRUCTURAL HETEROGENEITY OF 6 M GDMCL-DENATURED PROTEIN IS RELEVANT TO THE MODEL OF THE FOLDING LANDSCAPE

A widely accepted model of protein folding is illustrated by a funnel-shaped energy landscape (*50*−*52*). In this model, folding begins with diverse isomers of an unfolded protein. These isomers race down and navigate through a rugged folding funnel that comprises a large number of local minima, kinetic traps, and energy compartments, each of which is represented by a single transient conformational intermediate or a group of them (*53*, *54*). This funnel model appears to be consistent with and adaptable to the overwhelming majority of experimental data accumulated so far. It satisfactorily explains the two-state and multistate folding kinetics as well as the diverse complexity of folding intermediates observed experimentally with many different proteins.

The common use of 6 M GdmCl-denatured proteins as the starting materials of folding experiments is congruent with the funnel model, because most of them do comprise heterogeneous isomers. For instance, when folding of TAP is initiated with a 6 M GdmCl-denatured sample, the starting material consists of seven X-TAP isomers (Figure 3A); each adopts a unique extent of unfolding, and each navigates through its own rugged pathway to reach the native structure (*55*). Specifically, isomers X-TAP-**g** and X-TAP-**f** were found to act as major kinetic traps of TAP folding.

Alternatively, a folding experiment with TAP can be initiated with isolated X-TAP-**a**. In this approach, folding starts with a structurally (disulfide) defined isomer that possesses the highest free energy among all unfolded X-TAP isomers (*56*). The results (Figure 3B) show that the early stage of folding involves reorganization of the C-terminal domain, leading to the accumulation of isomer X-TAP-**d** as a major intermediate. This was followed by the formation of a major kinetic trap which

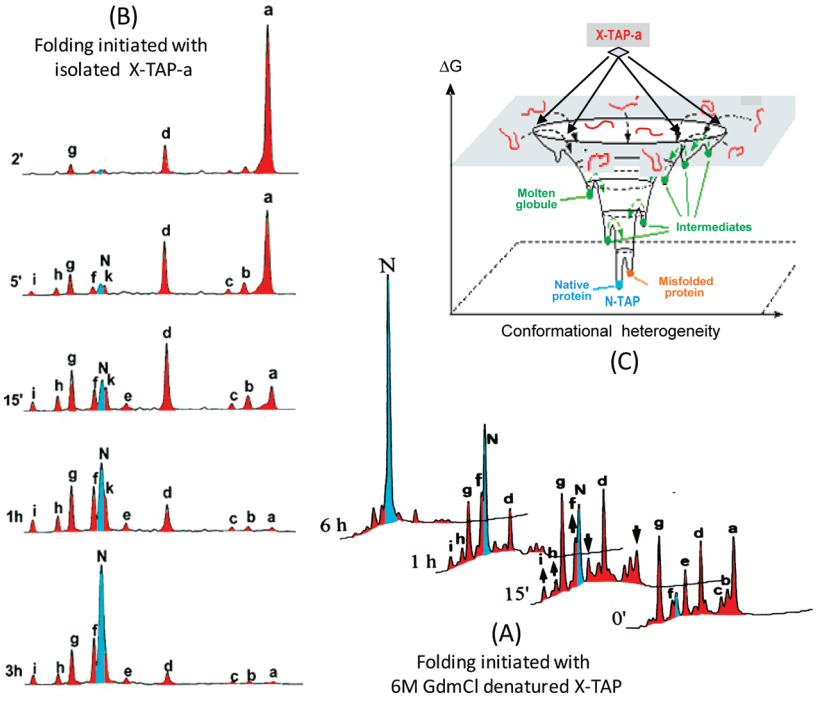

FIGURE 3: (A) Refolding initiated with 6 M GdmCl-denatured TAP via disulfide scrambling. N-TAP was denatured with 6 M GdmCl using the method of disulfide scrambling to form X-TAP isomers (Figure 1). They were purified by gel filtration, freeze-dried, and allowed to refold in Tris-HCl buffer (0.1 M, pH 8.4) containing 0.5 mM cysteine. Refolding intermediates were trapped by acidification and analyzed by HPLC. The starting material of folding comprises heterogeneous X-TAP isomers, and therefore, the folding landscape is illustrated by a funnel model. (B) Refolding initiated with isolated X-TAP-**a** via disulfide scrambling. HPLC-purified X-TAP-**a** was allowed to refold in Tris-HCl buffer (0.1 M, pH 8.4) containing 0.5 mM cysteine. Refolding intermediates were similarly trapped by acidification and analyzed by HPLC. Using this approach, the folding landscape is fittingly displayed as a diamond model, in which the conformational heterogeneity of TAP is reduced to a minimum at the two extreme ends of the energy landscape. (C) Funnel model and diamond model of the folding landscape. This figure is adapted from ref *53*.

comprises three X-TAP (**g**, **f**, and **k**) isomers sharing the same non-native disulfide bond (Cys^{15}−Cys^{33}) (Figure 1). The folding events of X-TAP-**a** demonstrate that the energy landscape of protein folding can be fittingly illustrated by a diamond model, in which the conformational heterogeneity of the protein is characterized by a bell-shaped curve against the descending free energy (Figure 3C). At the two extreme ends of the energy landscape, the conformational heterogeneity of the protein is reduced to a minimum. It reaches the maximum plateau approximately halfway through the folding. Indeed, unfolding of N-TAP to form X-TAP isomers (Figure 1) also follows the same shape of the energy landscape. A similar model of the energy landscape has been shown in the unfolding and refolding of α-lactalbumin (*41*, *42*) using the method of disulfide scrambling.

STRUCTURAL HETEROGENEITY OF 6 M GDMCL-DENATURED PROTEIN IS CRUCIAL TO THE EARLY STAGE OF THE FOLDING MECHANISM

The most crucial event in protein folding is what occurs during the earliest stage. It is also one of the poorly understood steps of protein folding (*37*). Two major models have been used to describe these events (*37*, *38*). The framework model proposes that nascent secondary structures (α-helix, β-strand, etc.) form first during the early stage of folding, which is followed by docking and packing of preformed secondary structural units to form the native tertiary structure. The model of hydrophobic collapse stipulates that a rapid hydrophobic collapse (interaction) accounts for the major driving force of early folding, which is followed by searching and fine-tuning of the conformation in a confined volume to reach the native structure.

Compelling and mounting experimental evidence supports both models (*28*−*36*). Nascent secondary structures and native-like hydrophobic clusters are indeed detected as early folding intermediates, and many of them are often observed at dead-time folding. However, the fact that many starting materials of folding experiments still contain residual structures raises the question of whether intermediates detected at the dead-time folding are results of the collapsed state or the unfolded state. In other words, are these intermediates derived from the fully unfolded state via dead-time burst phase collapse, or are they residual structures of the unfolded state that already exist at the starting point of folding? Answering this question will require the structural information for the unfolded state. If these structures are already present at the unfolded state, then they are actually unfolding intermediates instead of early folding intermediates. There is no guarantee that they will form (although they may) if the starting material of folding is homogeneous and fully unfolded. For example, the folding reaction of the cold shock protein from *Bacillus caldolyticus* (Bc-Csp) is preceded by a rapid chain collapse. However, FRET study has ruled out the possibility that the collapsed form is a folding intermediate with nativelike chain topology. It is better described as a mixture of compact conformations that belong to the unfolded state ensemble, with some of its structural elements that are reminiscent of the native protein (*28*).

Another example is illuminated here with the folding of lysozyme, which is one of the most extensively investigated models for elucidation of the mechanism of protein folding (*57*). Native lysozyme comprises 129 amino acids which are organized into two structural domains (α-helical domain and β-sheet domain) and stabilized by four disulfide bonds. The majority

Table 1: Structural Properties of 6 M GdmCl-Denatured Disulfide Proteins[a]

protein[b]	extent of denaturation[c] (%)	extent of unfolding[d] (%)	extent of heterogeneity[e] (%)
BPTI (58 amino acids, three disulfides)	< 2	< 1	not available
hirudin (65 amino acids, three disulfides)	60	ND[f]	43 (6/14)
EGF (53 amino acids, three disulfides)	87	ND[f]	43 (6/14)
TAP (60 amino acids, three disulfides)	95	23	50 (7/14)
C3a (77 amino acids, three disulfides)	> 96	33	29 (4/14)
PCI (39 amino acids, three disulfides)	> 96	ND[f]	43 (6/14)
LCI (67 amino acids, four disulfides)	> 96	35	8 (8/104)
αLA (122 amino acids, four disulfides)	> 96	16	17 (18/104)
LYZ (129 amino acids, four disulfides)	> 94	ND[f]	2 (2/104)

[a]All proteins were denatured using the method of disulfide scrambling (*28*, *29*). This was achieved by incubating the native protein in Tris-HCl buffer (pH 8.4) containing GdmCl (6 M) and β-mercaptoethanol (0.1−0.2 mM) for 16 h. Denatured X-isomers are separated and quantified by reversed phase HPLC. [b]BPTI is bovine pancreatic trypsin inhibitor (*44*). Hirudin is leech-derived thrombin inhibitor (*39*). EGF is human epidermal growth factor (*45*). TAP is tick anticoagulant peptide (*40*). C3a is anaphylatoxin (*46*). PCI is potato carboxypeptidase inhibitor (*47*). LCI is leech carboxypeptidase inhibitor (*48*). αLA is bovine α-lactalbumin (*41*). LYZ is hen lysozyme (*49*). In the case of lysozyme, the seven minor X-isomers were not included in the calculation. [c]The definition of denaturation is described in the text. Allowed deviation of ±5%. [d]The definition of unfolding is described in the text. Allowed deviation of ±5%. [e]The definition of heterogeneity is described in the text. [f]Not determined.

of these studies were initiated with 6 M GdmCl-denatured lysozyme without disruption of its four native disulfide bonds (disulfide intact). Specifically, folding of lysozyme was shown to use kinetically partitioned pathways (*58*−*60*). Approximately 75−85% of the unfolded lysozyme molecules refold on a slow track (τ = 420 ms) via well-populated, partially folded intermediates. The remaining 15−25% of the molecules refold by a fast track (τ = 50 ms) via a two-state process with few detectable intermediates. The origin of this kinetic partitioning has been a subject of discussion (*58*). The question is whether the heterogeneity of the collapsed state or the unfolded state provides a mechanism for generating these two kinetically distinct populations of folding molecules. Studies in the laboratories of Dobson (*60*) and Kiefhaber (*59*) have arrived at conclusions that favor the collapsed state.

Using the method of disulfide scrambling, we have found that 6 M GdmCl-denatured lysozyme comprises, among seven very minor isomers, two major populations of unfolded isomers, namely, X-LYZ-**a** and X-LYZ-**b** at a molar ratio of ~80:20 (Figure 4) (*49*). These two unfolded isomers can be isolated for a structural characterization and refolding experiment. X-LYZ-**a** and X-LYZ-**b** were shown to exist in equilibrium at the unfolded state. Their disulfide structures (Figure 4) and CD properties indicate that X-LYZ-**a** is more extensively unfolded than X-LYZ-**b**. For instance, X-LYZ-**b** still retains the two native disulfide bonds at the β-sheet domain. Refolding experiments using the method of disulfide scrambling also show that the folding rate of X-LYZ-**a** is ~8−10 times slower than that of

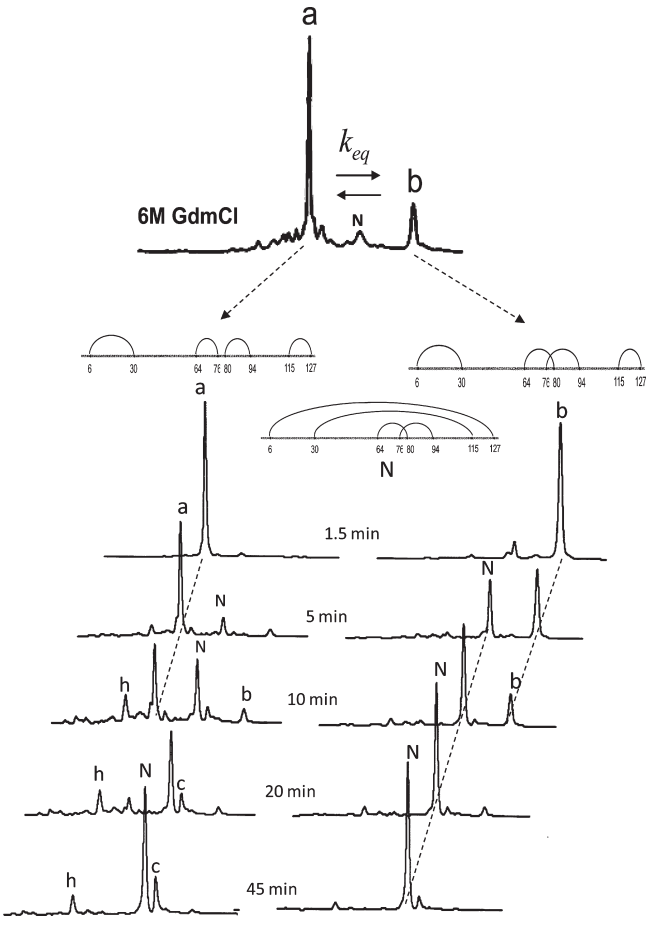

FIGURE 4: Refolding of two denatured lysozyme isomers using the method of disulfide scrambling. GdmCl (6 M)-denatured lysozyme comprises two major fractions of X-isomers, X-LYZ-**a** and X-LYZ-**b** (*49*). They were purified by HPLC and allowed to refold in Tris-HCl buffer (0.1 M, pH 8.4) containing β-mercaptoethanol (0.1 mM). Folding intermediates were trapped by acidification and analyzed by HPLC. The disulfide structures of N-LYZ, X-LYZ-**a**, and X-LYZ-**b** are given. The folding kinetics of X-LYZ-**a** is 8-fold slower than that of X-LYZ-**b**. Folding intermediates of X-LYZ-**a** are also more heterogeneous than that of X-LYZ-**b**.

X-LYZ-**b**, and folding intermediates of X-LYZ-**a** are far more heterogeneous than that of X-LYZ-**b** (Figure 4). These folding properties are strikingly similar to those observed with the conventional "disulfide intact" studies (*58*, *60*) and suggest that the slow and fast track of lysozyme folding likely originates from the conformational heterogeneity of the unfolded state. It needs to be mentioned that heat-denatured lysozyme comprises far more heterogeneous X-LYZ isomers (*49*). Consequently, the folding pathway of heat-unfolded lysozyme will likely differ significantly from that of 6 M GdmCl-unfolded lysozyme. Nonetheless, it remains to be demonstrated whether structures of 6 M GdmCl-denatured lysozyme generated by the disulfide intact and "disulfide scrambling" methods may resemble each other.

CONCLUDING REMARKS

Perhaps one of the most pressing needs and challenging tasks in studying protein folding is to develop methods that would ensure complete abolition of residual structures. This would enable preparation of fully unfolded protein as the starting material of folding experiments and facilitate interpretation of the formation of early folding intermediates. GdmCl and GdmSCN are among the most effective protein denaturants.

However, even with the most potent denaturing conditions currently available, many proteins still preserve residual structures. The extraordinary conformational stability of BPTI is one of the examples (*44*). The definition and criteria of complete protein unfolding will require universal consensus and may need to be verified by diverse physicochemical methods. The quandary is that attaining the state of complete unfolding may be as elusive as reaching absolute zero.

On an additional note, this author believes that ideal proteins to be investigated by the conformational folding experiments ought to be those devoid of disulfide bonds. It would be difficult to fully unfold a protein when its structure is constrained by native disulfide bonds. For disulfide-containing proteins, the folding mechanism is preferably investigated by the method of disulfide oxidation (*61*−*63*) or disulfide scrambling (*42*, *56*). The method of disulfide oxidation for studying protein folding (oxidative folding) was pioneered by Creighton and Scheraga in their seminal studies of BPTI (*61*, *64*−*66*) and ribonuclease A (*67*−*69*). Unlike the method of disulfide scrambling, oxidative folding is initiated with a fully reduced and denatured protein (designated as R-protein) (*62*), which was typically generated by reductive unfolding of the native protein in the presence of DTT and 6 M GdmCl. The method of disulfide scrambling is effectively derived from our earlier investigations of protein folding using the method of disulfide oxidation. In contrast to the oxidative folding pathway of BPTI which comprises intermediates that adopt almost exclusively native disulfide bonds (*65*, *66*), oxidative folding of many disulfide proteins was shown to undergo fully oxidized X-isomers comprising non-native disulfide bonds as essential folding intermediates. For instance, in the cases of oxidative folding of hirudin (*70*), potato carboxypeptidase inhibitor (*71*), and TAP (*55*), X-isomers formed rapidly during the early stage of folding. This was followed by the conversion of X-hirudin and X-TAP isomers via disulfide scrambling (shuffling) to attain the native hirudin and TAP. Extensive characterization of X-isomers subsequently led to the development of the disulfide scrambling technique for studying protein unfolding and refolding (*40*−*42*).

REFERENCES

1. Dill, K. A., Ozkan, S. B., Shell, M. S., and Weikl, T. R. (2008) The protein folding problem. *Annu. Rev. Biophys. 37*, 289–316.
2. Baldwin, R. L. (2008) The search for folding intermediates and the mechanism of protein folding. *Annu. Rev. Biophys. 37*, 1–21.
3. Fersht, A. R. (2008) From the first protein structures to our current knowledge of protein folding: Delights and scepticisms. *Nat. Rev. Mol. Cell Biol. 9*, 650–654.
4. Dill, K. A., Ozkan, S. B., Weikl, T. R., Chodera, J. D., and Voelz, V. A. (2007) The protein folding problem: When will it be solved? *Curr. Opin. Struct. Biol. 17*, 342–346.
5. Service, R. F. (2008) Problem solved* (*sort of). *Science 321*, 784–786.
6. Tanford, C. (1968) Protein denaturation. *Adv. Protein Chem. 23*, 121–282.
7. Tanford, C. (1970) Protein denaturation. C. Theoretical models for the mechanism of denaturation. *Adv. Protein Chem. 24*, 1–95.
8. Yi, Q., Scalley-Kim, M. L., Alm, E. J., and Baker, D. (2000) NMR characterization of residual structure in the denatured state of protein L. *J. Mol. Biol. 299*, 1341–1351.
9. Neri, D., Billeter, M., Wider, G., and Wuthrich, K. (1992) NMR determination of residual structure in a urea-denatured protein, the 434-repressor. *Science 257*, 1559–1563.
10. McCarney, E. R., Kohn, J. E., and Plaxco, K. W. (2005) Is there or isn't there? The case for (and against) residual structure in chemically denatured proteins. *Crit. Rev. Biochem. Mol. Biol. 40*, 181–189.
11. Shortle, D., and Abeygunawardana, C. (1993) NMR analysis of the residual structure in the denatured state of a mutant of staphylococcal nuclease. *Structure 1*, 121–134.
12. Hammack, B. N., Smith, C. R., and Bowler, B. E. (2001) Denatured state thermodynamics: Residual structure, chain stiffness and scaling factors. *J. Mol. Biol. 311*, 1091–1104.
13. Smith, L. J., Fiebig, K. M., Schwalbe, H., and Dobson, C. M. (1996) The concept of a random coil. Residual structure in peptides and denatured proteins. *Folding Des. 1*, R95–R106.
14. Gorovits, B. M., Seale, J. W., and Horowitz, P. M. (1995) Residual structure in urea-denatured chaperonin GroEL. *Biochemistry 34*, 13928–13933.
15. Shortle, D., and Ackerman, M. S. (2001) Persistence of native-like topology in a denatured protein in 8 M urea. *Science 293*, 487–489.
16. Englander, S. W., and Mayne, L. (1992) Protein folding studied using hydrogen-exchange labeling and two-dimensional NMR. *Annu. Rev. Biophys. Biomol. Struct. 21*, 243–265.
17. Shortle, D. R. (1996) Structural analysis of non-native states of proteins by NMR methods. *Curr. Opin. Struct. Biol. 6*, 24–30.
18. Dyson, H. J., and Wright, P. E. (2004) Unfolded proteins and protein folding studied by NMR. *Chem. Rev. 104*, 3607–3622.
19. Wong, K. B., Clarke, J., Bond, C. J., Neira, J. L., Freund, S. M., Fersht, A. R., and Daggett, V. (2000) Towards a complete description of the structural and dynamic properties of the denatured state of barnase and the role of residual structure in folding. *J. Mol. Biol. 296*, 1257–1282.
20. Religa, T. L., Markson, J. S., Mayor, U., Freund, S. M., and Fersht, A. R. (2005) Solution structure of a protein denatured state and folding intermediate. *Nature 437*, 1053–1056.
21. Sari, N., Alexander, P., Bryan, P. N., and Orban, J. (2000) Structure and dynamics of an acid-denatured protein G mutant. *Biochemistry 39*, 965–977.
22. Russell, B. S., Melenkivitz, R., and Bren, K. L. (2000) NMR investigation of ferricytochrome c unfolding: Detection of an equilibrium unfolding intermediate and residual structure in the denatured state. *Proc. Natl. Acad. Sci. U.S.A. 97*, 8312–8317.
23. Wirmer, J., Berk, H., Ugolini, R., Redfield, C., and Schwalbe, H. (2006) Characterization of the unfolded state of bovine α-lactalbumin and comparison with unfolded states of homologous proteins. *Protein Sci. 15*, 1397–1407.
24. Alexandrescu, A. T., Evans, P. A., Pitkeathly, M., Baum, J., and Dobson, C. M. (1993) Structure and dynamics of the acid-denatured molten globule state of α-lactalbumin: A two-dimensional NMR study. *Biochemistry 32*, 1707–1718.
25. Pearce, M. C., Cabrita, L. D., Rubin, H., Gore, M. G., and Bottomley, S. P. (2004) Identification of residual structure within denatured antichymotrypsin: Implications for serpin folding and misfolding. *Biochem. Biophys. Res. Commun. 324*, 729–735.
26. Marsh, J. A., Neale, C., Jack, F. E., Choy, W. Y., Lee, A. Y., Crowhurst, K. A., and Forman-Kay, J. D. (2007) Improved structural characterizations of the drkN SH3 domain unfolded state suggest a compact ensemble with native-like and non-native structure. *J. Mol. Biol. 367*, 1494–1510.
27. Ropson, I. J., Boyer, J. A., and Dalessio, P. M. (2006) A residual structure in unfolded intestinal fatty acid binding protein consists of amino acids that are neighbors in the native state. *Biochemistry 45*, 2608–2617.
28. Magg, C., Kubelka, J., Holtermann, G., Haas, E., and Schmid, F. X. (2006) Specificity of the initial collapse in the folding of the cold shock protein. *J. Mol. Biol. 360*, 1067–1080.
29. Welker, E., Maki, K., Shastry, M. C., Juminaga, D., Bhat, R., Scheraga, H. A., and Roder, H. (2004) Ultrarapid mixing experiments shed new light on the characteristics of the initial conformational ensemble during the folding of ribonuclease A. *Proc. Natl. Acad. Sci. U.S.A. 101*, 17681–17686.
30. Agashe, V. R., Shastry, M. C., and Udgaonkar, J. B. (1995) Initial hydrophobic collapse in the folding of barstar. *Nature 377*, 754–757.
31. Camilloni, C., Sutto, L., Provasi, D., Tiana, G., and Broglia, R. A. (2008) Early events in protein folding: Is there something more than hydrophobic burst? *Protein Sci. 17*, 1424–1433.
32. Felitsky, D. J., Lietzow, M. A., Dyson, H. J., and Wright, P. E. (2008) Modeling transient collapsed states of an unfolded protein to provide insights into early folding events. *Proc. Natl. Acad. Sci. U.S.A. 105*, 6278–6283.
33. Bilsel, O., and Matthews, C. R. (2006) Molecular dimensions and their distributions in early folding intermediates. *Curr. Opin. Struct. Biol. 16*, 86–93.
34. Kimura, T., Akiyama, S., Uzawa, T., Ishimori, K., Morishima, I., Fujisawa, T., and Takahashi, S. (2005) Specifically collapsed intermediate in the early stage of the folding of ribonuclease A. *J. Mol. Biol. 350*, 349–362.

35. Maki, K., Cheng, H., Dolgikh, D. A., Shastry, M. C., and Roder, H. (2004) Early events during folding of wild-type staphylococcal nuclease and a single-tryptophan variant studied by ultrarapid mixing. *J. Mol. Biol. 338*, 383–400.
36. Ferguson, N., and Fersht, A. R. (2003) Early events in protein folding. *Curr. Opin. Struct. Biol. 13*, 75–81.
37. Baldwin, R. L. (1989) How does protein folding get started? *Trends Biochem. Sci. 14*, 291–294.
38. Daggett, V., and Fersht, A. R. (2003) Is there a unifying mechanism for protein folding? *Trends Biochem. Sci. 28*, 18–25.
39. Chang, J.-Y. (1995) The properties of scrambled hirudins. *J. Biol. Chem. 270*, 25661–25666.
40. Chang, J.-Y (1999) Denatured states of tick anticoagulant peptide. Compositional analysis of unfolded scrambled isomers. *J. Biol. Chem. 274*, 123–128.
41. Chang, J.-Y., and Li, L. (2001) The structure of denatured α-lactalbumin elucidated by the technique of disulfide scrambling: Fractionation of conformational isomers of α-lactalbumin. *J. Biol. Chem. 276*, 9705–9712.
42. Chang, J.-Y. (2002) The folding pathway of α-lactalbumin elucidated by the technique of disulfide scrambling. *J. Biol. Chem. 277*, 120–126.
43. Lim-Wilby, M. S. L., Hallenga, K., De Maeyer, M., Lasters, I., Vlasuk, G. P., and Brunck, T. K. (1995) NMR structure determination of tick anticoagulant peptide. *Protein Sci. 4*, 178–186.
44. Chang, J.-Y., and Ballatore, A. (2000) The structure of denatured bovine pancreatic trypsin inhibitor (BPTI). *FEBS Lett. 473*, 183–187.
45. Chang, J.-Y., and Li, L. (2002) The Disulfide Structure of Denatured Epidermal Growth Factor: Preparation of scrambled disulfide isomers. *J. Protein Chem. 21*, 203–213.
46. Chang, J.-Y., Lin, C.-J., Salamanca, S., Pangburn, M. K., and Wetsel, R. A. (2009) Denaturation and Unfolding of Human Anaphylatoxin C3a: An unusually low covalent stability of its native disulfide bonds. *Arch. Biochem. Biophys.* (in press).
47. Chang, J.-Y., Li, L., Canals, F., and Aviles, F. X. (2000) The unfolding pathway and conformational stability of potato carboxypeptidase inhibitor. *J. Biol. Chem. 275*, 14205–14211.
48. Salamanca, S., Virtudes, V., Vendrell, J., Li, L., Aviles, F. X., and Chang, J.-Y. (2002) The unfolding pathway of leech carboxypeptidase inhibitor. *J. Biol. Chem. 277*, 17538–17543.
49. Chang, J.-Y., and Li, L. (2002) The unfolding pathway and structures of denatured lysozyme. *FEBS Lett. 511*, 73–78.
50. Onuchic, J. N., Wolynes, P. G., Luthey-Schulten, Z., and Socci, N. D. (1995) Toward an outline of the topography of a realistic protein-folding funnel. *Proc. Natl. Acad. Sci. U.S.A. 92*, 3626–3630.
51. Socci, N. D., Onuchic, J. N., and Wolynes, P. G. (1998) Protein folding mechanisms and the multidimensional folding funnel. *Proteins 32*, 136–158.
52. Dill, K. A., and Chan, H. S. (1997) From Levinthal to pathways to funnels. *Nat. Struct. Biol. 4*, 10–18.
53. Schultz, C. P. (2000) Illuminating folding intermediates. *Nat. Struct. Biol. 7*, 7–10.
54. Radford, S. E. (2000) Protein folding: Progress made and promises ahead. *Trends Biochem. Sci. 25*, 611–618.
55. Chang, J.-Y. (1996) The disulfide folding pathway of tick anticoagulant peptide, a Kunitz-type inhibitor structurally homologous to BPTI. *Biochemistry 35*, 11702–11709.
56. Chang, J.-Y., and Li, L. (2005) Divergent Folding Pathways of Two Homologous Proteins, BPTI and Tick Anticoagulant Peptide. *Arch. Biochem. Biophys. 437*, 85–95.
57. Matagne, A., and Dobson, C. M. (1998) The folding process of hen lysozyme: A perspective from the 'new view'. *Cell. Mol. Life Sci. 54*, 363–371.
58. Kiefhaber, T. (1995) Kinetic traps in lysozyme folding. *Proc. Natl. Acad. Sci. U.S.A. 92*, 9029–9033.
59. Wildegger, G., and Kiefhaber, T. (1997) Three-state model for lysozyme folding: Triangular folding mechanism with an energetically trapped intermediate. *J. Mol. Biol. 270*, 294–304.
60. Matagne, A., Radford, S. E., and Dobson, C. M. (1997) Fast and slow tracks in lysozyme folding: Insight into the role of domains in the folding process. *J. Mol. Biol. 267*, 1068–1074.
61. Creighton, T. E. (1978) Experimental studies of protein folding and unfolding. *Prog. Biophys. Mol. Biol. 33*, 231–297.
62. Creighton, T. E. (1986) Disulfide bonds as probes of protein folding pathways. *Methods Enzymol. 131*, 83–106.
63. Arolas, J. L., Aviles, F. X., Chang, J.-Y., and Ventura, S. (2006) Folding of small disulfide-rich proteins: Clarifying the puzzle. *Trends Biochem. Sci. 31*, 292–301.
64. Creighton, T. E. (1992) The disulfide folding pathway of BPTI. *Science 256*, 111–114.
65. Goldenberg, D. P. (1992) Native and non-native intermediates in the BPTI folding pathway. *Trends Biochem. Sci. 17*, 257–261.
66. Weissman, J. S., and Kim, P. S. (1991) Re-examination of the folding of BPTI: Predominance of native intermediates. *Science 253*, 1386–1393.
67. Konishi, Y., Ooi, T., and Scheraga, H. A. (1981) Regeneration of ribonuclease A from the reduced protein, isolation and identification of intermediates, and equilibrium treatment. *Biochemistry 20*, 3945–3955.
68. Narayan, M., Welker, E., Wedemeyer, W. J., and Scheraga, H. A. (2000) Oxidative Folding of Proteins. *Acc. Chem. Res. 33*, 805–812.
69. Scheraga, H. A., Wedemeyer, W. J., and Welker, E. (2001) Bovine pancreatic ribonuclease A: Oxidative and conformational folding studies. *Methods Enzymol. 341*, 189–221.
70. Chang, J.-Y. (1994) Controlling the speed of hirudin folding. *Biochem. J. 300*, 643–650.
71. Chang, J.-Y., Canals, F., Schindler, P., Querol, E., and Aviles, F. X. (1994) The disulfide folding pathway of potato carboxypeptidase inhibitor. *J. Biol. Chem. 269*, 22087–22094.